

Active damping of torsional vibrations in the drive train of a DFIG wind turbine

L. Chen¹, H. Xu^{1,2} and J. Wenske¹

¹ Fraunhofer Institute for Wind Energy and Energy System Technology,
 Am Seedeich 45, Bremerhaven, 27572, Germany

Phone/Fax number: +49 471 14290401, e-mail: liang.chen@iwes.fraunhofer.de, jan.wenske@iwes.fraunhofer.de

² Institute of Electrical Engineering, Chinese Academy of Sciences,
 No.6 Beiertiao, Zhongguancun, Beijing, 100190, China
 e-mail: xuhaocas@gmail.com

Abstract. Torsional vibrations in the drive train of the doubly-fed induction generator (DFIG) based wind turbine can cause large mechanical stress and reduce the life cycle of the components. They can be easily induced by sudden changes from the turbine rotor side or grid side. In this paper, a model-based active damper of the torsional vibration designed with the linear-quadratic-Gaussian (LQG) algorithm is proposed. The modelling of the drive train takes the flexibility of the rotor blades into account and utilizes a three-mass model. A combination of different simulation packages, namely FAST (Fatigue, Aerodynamics, Structure, Turbulence) and Matlab/Simulink describing important dynamics of both the mechanical and electrical side, is applied to analyse the vibrations in the drive train and test the algorithm. Simulation results show that the proposed active damping can suppress the torsional vibrations in the drive train effectively even if a grid fault occurs.

Key words

Torsional vibration, Active damping, Drive train, DFIG, LQG control

1. Introduction

Wind turbines based on DFIG are the most installed wind energy generation systems due to the high energy efficiency and low cost. Since the stator of the DFIG is directly connected to the grid, sudden changes from turbine rotor or grid side, such as wind gusts or voltage sags, can induce torsional vibrations in the drive train. They cause large mechanical stress and lead to reduction of lifetime of components. According to [1] gearbox-related failures are responsible for over 20% of downtime of the wind turbines. They usually need replacement only after 6–8 years. It is necessary to take some measures to mitigating torsional oscillations. For the wind turbines in MW range it is difficult to increase enough damping mechanically, in spite of the additional cost involved. A common solution to this problem is bandpass filters (BPF)

[2]-[3]. The generator speed is fed to the BPF for generating a torque ripple with the torsional frequency and an appropriate phase. This ripple is added to the torque command value and then the torsional vibration can be compensated. However, if the vibration is induced by the grid fault, which is much larger than the one induced by wind variations, the BPF is not able to compensate it effectively [4].

This paper gives an alternative solution, which works even in the case of a grid fault. The main idea is that the torsional vibration can be suppressed by eliminating the speed difference between the turbine rotor and generator, if they are referred to the same side of the gearbox (e.g. in the low speed side). The LQG control algorithm with the drive train model is employed for achieving better control performance. To validate the method a sophisticated wind turbine model for simulation is built in Matlab/Simulink. The aerodynamics and structure dynamics of the turbine is modelled with the FAST, which has an interface to Matlab/Simulink. The electrical parts of the turbine, including the generator, control system, power electronics, protection systems and the grid, are modelled directly with Simulink, as shown in Fig. 1. Then all details of the turbine in both mechanical and electrical parts are simulated. Simulations show that the proposed method can effectively suppress torsional vibrations even in the worst-case, i.e., the turbine is loaded with rated torque before a low voltage ride through (LVRT) event with a voltage sag of 100%.

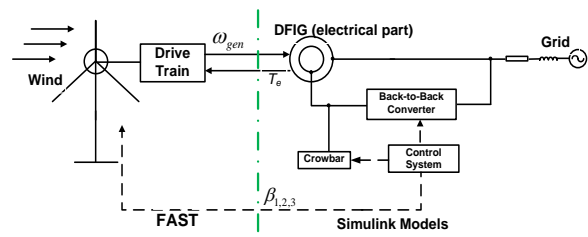


Fig. 1. The simulation structure of a DFIG

This paper is organized as follows: in section 2 the complete wind turbine model is introduced in detail. Section 3 introduces the LQG based active damping strategy. Then simulation results are shown in section 4. At last the conclusion is conducted in section 5.

2. Wind Turbine Model

A. Mechanical model based on FAST

FAST is a comprehensive aeroelastic simulation code and is capable of predicting both extreme and fatigue loads of two- and three-bladed horizontal-axis wind turbines [5]-[6], which is developed by NREL (National Renewable Energy Laboratory). The core of this code is an advanced model for flexible structure of the wind turbines, taking the flexibility of the tower, blades and other components of the wind turbines into account.

In this research, FAST has been used to model a wind turbine, considering 16 DOFs (degree of freedom) including first and second flapwise blade mode, edgewise blade mode, drive-train rotational flexibility, yaw angle, first and second tower fore-aft bending mode, first and second tower side-side bending mode, and generator azimuth angle. To define a typical large wind turbine, the NREL 5-MW baseline turbine [7] is utilized, which is widely used and accepted for the research purpose. The basic parameters are listed in Table I.

Table I. – NREL 5MW Wind Turbine

Power rating	5 MW
Rotor	3-bladed, upwind
Control	variable speed, pitch
Rotor diameter	126m
Hub height	90m
Rated, cut-out wind speed	11.4m/s, 25m/s
Rated rotor speed	12.1rpm
Total rotor inertial ($J_1 + J_2$)	$3.09 \times 10^7 \text{kgm}^2$
Gearbox ratio	97:1
Equivalent shaft stiffness (K_{23})	$8.676 \times 10^8 \text{Nm/rad}$
Equivalent shaft damping (D_{23})	$6.215 \times 10^6 \text{Nms/rad}$

B. Electrical part model based on Simulink

Although FAST contains detailed models in the aspects of aerodynamics and structural dynamics of a wind turbine. The models of electrical components and controller are very simplified. Because FAST offers an interface to Matlab/Simulink, the electrical parts including controllers are modelled by Simulink blocks.

1) DFIG subsystem

The electrical model of the DFIG is basically a wound rotor induction machine. It is expressed in a d-q reference frame. The dynamics of the induction machine can be written as [8]. (Stator and rotor equation are both based on motor convention, taking positive currents going into the machine.):

$$v_{ds} = R_s i_{ds} + \dot{\lambda}_{ds} - \omega_s \lambda_{qs} \quad (1)$$

$$v_{qs} = R_s i_{qs} + \dot{\lambda}_{qs} + \omega_s \lambda_{ds} \quad (2)$$

$$v_{dr} = R_r i_{dr} + \dot{\lambda}_{dr} - (\omega_s - \omega_r) \lambda_{qr} \quad (3)$$

$$v_{qr} = R_r i_{qr} + \dot{\lambda}_{qr} + (\omega_s - \omega_r) \lambda_{dr} \quad (4)$$

The flux and current relations are given as

$$\lambda_{ds} = L_s i_{ds} + L_m i_{dr} \quad (5)$$

$$\lambda_{qs} = L_s i_{qs} + L_m i_{qr} \quad (6)$$

$$\lambda_{dr} = L_r i_{dr} + L_m i_{ds} \quad (7)$$

$$\lambda_{qr} = L_r i_{qr} + L_m i_{qs} \quad (8)$$

The generator torque is expressed as

$$T_e = 1.5 p (\lambda_{ds} i_{qs} - \lambda_{qs} i_{ds}),$$

where

d, q direct and quadrature axis;
 s, r stator and rotor variables;
 R_s, R_r stator, rotor resistance;
 L_s, L_r, L_m stator, rotor and magnetizing inductances;
 ω_s, ω_r stator and rotor angular electrical speed;
 p number of pole pairs.

All rotor-side variables and parameters above are referred to the stator. Here the d-q frame is aligned with the stator voltage. The stator resistance is very small and can be ignored. Then the generator torque can be formulated by

$$T_e = -\frac{3pL_m}{2\omega_s L_s} i_{dr} v_{ds}. \quad (9)$$

The parameters of DFIG used in this study are given in Table II.

Table II. – DFIG Parameters

Rated voltage (line to line)	960V
Equivalent inertia of generator and gearbox (J_3)	$5.03 \times 10^6 \text{kgm}^2$
R_s	2.1mΩ
R_r	2.1mΩ
L_s	4.413mH
L_r	4.409mH
L_m	4.26mH
p	3

2) Control system

In this paper wind turbine control system includes pitch controller and generator torque controller. The yaw control is ignored. The basic control objectives are to optimize the power production in the case of partial load (below the rated wind speed) and to limit the aerodynamic power in the case of full load (above the rated wind speed).

If the turbine runs under rated power, the generator speed is adjusted by regulating the generator torque to follow an optimal torque versus speed curve. The optimal generator torque is proportional to the square of the generator speed.

If the turbine runs with or above the rated wind speed, the generator torque is held constant at the rated value and the power and speed of the turbine are limited by controlling the pitch angle. For the safety and stability of the turbine the pitch system usually has a time constant T_{servo} between 0.2s and 0.3s, as shown in Fig. 2, in which

β stands for the pitch angel. Thus, even if the frequency of the torsional vibration is slow as 1Hz it is difficult for the pitch system to handle the torsional vibration. In this paper the pitch actuator is modelled by a first order lag with a time constant of 0.2s with limiters of both pitch angle and change rate.

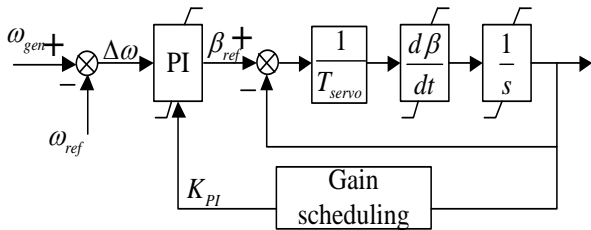


Fig. 2. The pitch system

3) Converter system

A back-to-back converter system is used to connect the DFIG rotor to the grid, as shown in the Fig. 3. The rotor-side and grid-side converter have a common DC-bus. A DC-bus capacitor is employed to stabilize the DC voltage. A chopper is also added to eliminate small fluctuations of the DC voltage. The DFIG is controlled by the rotor-side converter. Meanwhile the active and reactive power of the stator is controlled indirectly by means of the inner rotor current control loop. The control is performed field oriented, where the rotor current loop is stator voltage or flux orientated. The grid-side converter controls the DC link voltage to be constant and may also control the active and reactive power taken from or transferred to the grid. In this paper the converter system is simulated by the average model with the space vector PWM modulation for investigating the impact of the electrical components on the drive train, especially during and after a grid event. The detailed modelling principle can be found in [9].

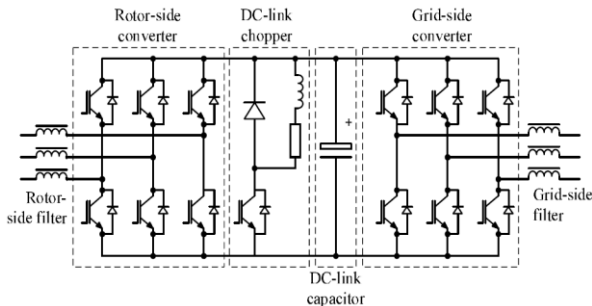


Fig. 3. The structure of the converter system [10]

4) Crowbar

Nowadays the fault ride through ability becomes a basic requirement for a modern DFIG wind turbine. The new grid codes force wind turbines to stay connected to the grid during and after a voltage dip, i.e., low voltage ride through (LVRT). The conventional way to protect a DFIG wind turbine from a grid fault is by installing crowbar devices [11]-[12]. The crowbar is capable of limiting the overvoltage in the DC-Link and overcurrent in the rotor-side converter. However, the rotor circuit of the DFIG has to be shorted by the crowbar during the grid fault which turns the DFIG into a conventional induction machine. During generator mode transition, the generator is not controllable and the torque begins to oscillate. Furthermore this oscillation will be transferred to the drive train.

Therefore, it is necessary to include the crowbar device into a DFIG model for the vibration analysis.

The crowbar modelled as a symmetric three phase y-connected resistance R_{crow} . If the crowbar is activated, the rotor of the DFIG is switched from the rotor-side converter to the external resistors R_{crow} . The rotor-side converter is bypassed and can be protected. If the grid fault is cleaned, the crowbar is switched off and the rotor-side converter is connected with generator again. According to [13], small resistance values lead to high current and torque transient peaks at the fault moment, while a very high crowbar resistance can imply a risk of excessive rotor current, torque and reactive power transients when crowbar is removed. In this paper, a constant resistance value of $80R_r$ will be used as an appropriate trade-off.

The crowbar cannot be switched arbitrarily. The switch rules are very complicated and are out of the focus of this paper. In our simulation the operation of the crowbar is simply controlled by the time.

5) Grid Model

The grid is represented by a Thevenin equivalent model, which consists of three voltage sources connected with their impedance in series. To simulate the voltage dip, a voltage step with duration of 150ms, is applied to the voltage source.

3. Model-based Active Damping

Large torsional torque will be expected due to weak structure damping and sudden changes from turbine rotor and grid side. Here a model-based active damper is designed with the LQG algorithm to adjust the generator torque for mitigating torsional variations.

A. Equivalent model of the drive train

In earlier work, a two-mass model was usually used to represent the drive train mechanical system, which takes into account only the shafts flexibilities and assumes that the blades are rigid. The drive train is represented by two inertias, i.e., one represents the turbine rotor and the other stands for the generator and gearbox. The rest of the drive train is considered as massless. However, the rotor of modern wind turbine is large and long and cannot be simply considered as a rigid body. In the study of electrical transient performance, it is also important to consider the turbine rotor dynamics [14]-[15]. The reason is that the blade edgewise symmetrical mode couples directly to the drive train so if this mode is excited it will also lead to the torsional vibration.

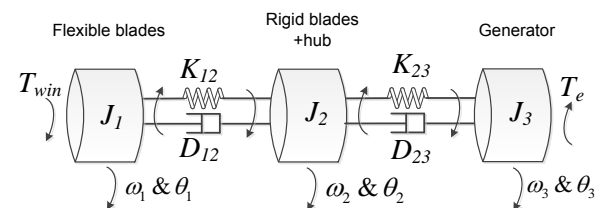


Fig. 4. The equivalent model of the drive train Hence a three-mass model, which considers both flexibilities of drive train shaft and rotor edgewise, is

employed as shown in Fig. 4. Where J_1 represents the inertia of the effective flexible part of the blades; J_2 represents the inertia of the hub and the rigid part of the blades; J_3 stands for the equivalent inertia of the generator and gearbox. K_{12} represents the effective blade stiffness. K_{23} is the equivalent shaft stiffness referred to the low speed side. D_{12} , D_{23} are the damping coefficients. $\theta_{1,2,3}$ and $\omega_{1,2,3}$ represent the rotation angle and rotation angular speed of the three inertias respectively. T_{win} and T_e represent the aerodynamic and generator torque. The dynamics referred to the low-speed shaft (LSS) is given by equations (10)-(14).

$$J_1 \dot{\omega}_1 = T_{win} - K_{12}(\theta_1 - \theta_2) - D_{12}(\omega_1 - \omega_2) \quad (10)$$

$$J_2 \dot{\omega}_2 = K_{12}(\theta_1 - \theta_2) + D_{12}(\omega_1 - \omega_2) - K_{23}(\theta_2 - \theta_3) - D_{23}(\omega_2 - \omega_3) \quad (11)$$

$$J_3 \dot{\omega}_3 = K_{23}(\theta_2 - \theta_3) + D_{23}(\omega_2 - \omega_3) - N \cdot T_e \quad (12)$$

$$\dot{\theta}_1 - \dot{\theta}_2 = \omega_1 - \omega_2 \quad (13)$$

$$\dot{\theta}_2 - \dot{\theta}_3 = \omega_2 - \omega_3, \quad (14)$$

Where N is the gearbox ratio.

The natural frequencies of torsional vibration f_1 , f_2 of the three-mass model are given by (15):

$$f_{1,2} = \frac{1}{2\pi} \left(-\frac{b}{2} \pm \sqrt{\frac{b^2}{4} - 4c} \right)^{0.5}, \quad (15)$$

where

$$b = -[K_{12}(\frac{1}{J_1} + \frac{1}{J_2}) + K_{23}(\frac{1}{J_2} + \frac{1}{J_3})]$$

and

$$c = K_{12}K_{23}(\frac{J_1 + J_2 + J_3}{J_1 J_2 J_3}).$$

In this three-mass model the parameters J_1 , J_2 and K_{12} are unknown. But they can be derived if f_1 and f_2 are known. Simulations are carried out to identify f_1 and f_2 . The worst-case scenario is considered here. Three dimensional turbulent wind has been used for simulating inflow turbulence environments which is produced by Turbsim [16]. The three phase 100% voltage dip occurs at $t=7s$ with the duration of 150ms simulated by a voltage step of the voltage source in the grid model. The crowbar is activated at $t=7.002s$ and switched off at $t=7.152s$. The load in the drive train, which is represented by the LSS torque, is shown in Fig. 5.

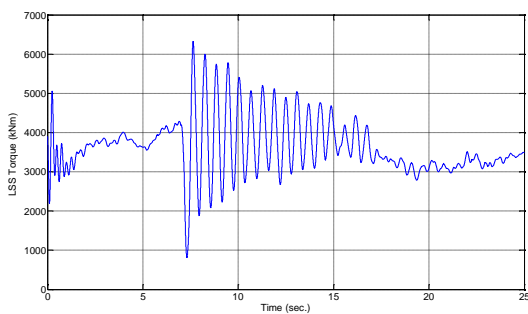


Fig. 5. The LSS torque with a LVRT event

According to the power spectral density (PSD) analysis of LSS torque, shown in Fig. 6, two dominant oscillation frequencies can be extracted at about 1.7Hz and 4Hz, while the torsional frequency according to the two-mass

model would be about 2.2Hz. It also implies that it is necessary to model the drive train with a three-mass model.

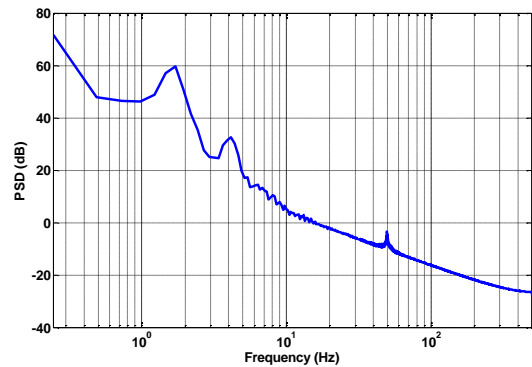


Fig. 6. PSD of the LSS torque

B. Active Damping with LQG

Fig. 7 shows the schematic of the proposed control strategy. The controller is designed to compensate the torsional vibration in the drive train by the modification of reference of the generator torque.

$$T_e^* = T_{bc} + T_{da}. \quad (16)$$

Where T_{bc} is the basic torque control reference calculated from the torque-speed curve. T_{da} is the damping torque derived by the LQG, which is simply the combination of a linear-quadratic regulator (LQR) and a Kalman filter.

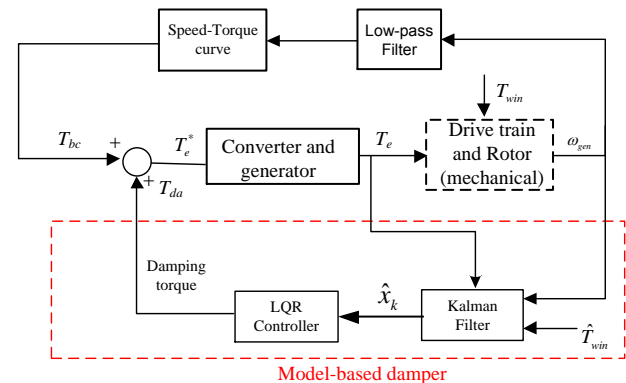


Fig. 7. The generator control with the LQG damper

The linear drive train model developed from (10-14) can be expressed in the state space form as:

$$\begin{cases} \dot{x} = Ax + Bu + B_d u_d \\ y = Cx \end{cases} \quad (17)$$

x is a vector consisting of five system states:

$$x = [\omega_1 - \omega_2 \quad \theta_1 - \theta_2 \quad \omega_2 - \omega_3 \quad \theta_2 - \theta_3 \quad \omega_3]^T.$$

u represents the control input T_{da} and u_d is the disturbance input T_{win} . ω_3 is the generator speed, which is the only measurement of the system (17). The other matrices and vectors are shown in the following:

$$B = \begin{bmatrix} 0 & 0 & \frac{N}{J_3} & 0 & -\frac{N}{J_3} \end{bmatrix}^T,$$

$$B_d = \begin{bmatrix} \frac{1}{J_1} & 0 & 0 & 0 & 0 \end{bmatrix}^T,$$

$$C = [0 \ 0 \ 0 \ 0 \ 1],$$

$$A = \begin{bmatrix} 0 & -\frac{K_{12}}{J_1} - \frac{K_{12}}{J_2} & 0 & \frac{K_{23}}{J_2} & 0 \\ 1 & 0 & 0 & 0 & 0 \\ 0 & \frac{K_{12}}{J_2} & 0 & -\frac{K_{23}}{J_2} - \frac{K_{23}}{J_3} & 0 \\ 0 & 0 & 1 & 0 & 0 \\ 0 & 0 & 0 & \frac{K_{23}}{J_3} & 0 \end{bmatrix}.$$

Because the damping factors are very small and usually unknown, they are assumed to be zero here. It actually makes the active damping of the model is more difficult than the real plant.

The LQR algorithm usually uses a performance index J to define the controller objectives, which is a quadratic function and can be expressed as:

$$J = \int_0^{\infty} [x^T(t)Qx(t) + u^T(t)Ru(t)] dt. \quad (18)$$

Where Q is a symmetric, positive semi-definite weighting matrix on the states that satisfies the algebraic Riccati equation (ARE) and R is a symmetric, positive definite weighting on the control input. The matrices are adjusted based on a trade-off between high control performance (large Q) and low control output (large R). For the simplicity they are usually set as diagonal. With the LQR theory if the optimal input can be found, the index function J can be minimized, which means all state variables will tend to zero. In our case only the states x_1 and x_3 should be controlled to zero so they have much larger weighting factors than others. The appropriate Q and R can be obtained by running simulations.

The LQR needs all information of the system. A discrete Kalman filter is used here, which is robust to measurement and system noises. It makes a one-step-ahead prediction of the states, and also estimates what the measured output would be. A correction updates the state estimates, taking into account the prediction error. The algorithm is iterative and the correction factor, Kalman gain K_k , updates at every iteration. Assuming the stochastic disturbances acting on the system are Gaussian, K_k is derived from the system dynamics to minimize the expected sum of squares of the prediction error. For reducing the online computational cost the stationary Kalman filter is applied, which means the Kalman gain is constant. Thus the estimator has the structure as shown in (19)

$$\hat{x}_{k+1} = \hat{x}_k + K_k (y_k - \hat{y}_k). \quad (19)$$

Where y_k stands for the measurement.

The system is subject to the unknown input T_{win} . It is approximated by

$$\hat{T}_{win} \approx T_e + (J_1 + J_2)\hat{\omega}_{gen}, \quad (20)$$

where $\hat{\omega}_{gen}$ is the numerical differentiation of the generator speed filtered by a first order lowpass filter.

4. Simulation

The proposed active damper is tested by simulations. The test scenario is same as described in the section 3. Multiple

sampling times are applied. The smallest sampling time is 0.25ms, which is the sampling time of the space vector PWM modulation. The measurement and controllers work with 1ms and 5ms, respectively. The FAST has two time constants for integrations, 10ms for the aerodynamics and 5ms for the structure dynamics. Then good balance between the accuracy and simulation time can be achieved. The damping torque T_{da} is limited by 10% of the rated torque. Furthermore, the proposed LQG damper is also compared with the conventional two-mass model based LQG.

Fig. 8 shows the speed of the generator. The speed with active damping oscillated much less. There are not so much differences of damping performance of two-mass and three-mass mass model.

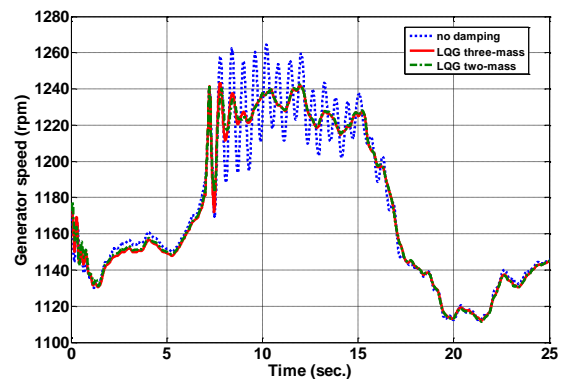


Fig. 8. Generator speeds with/without damping

The characteristics of the loads in the drive train in time domain and frequency domain are shown in Fig 9. and Fig.10., respectively. It can be observed that the LSS torque also oscillated significantly less if the damping torque was activated. But according to the PSD in Fig. 10

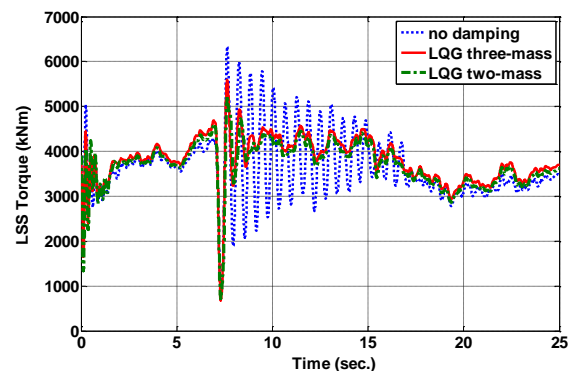


Fig. 9. LSS torques with/without damping

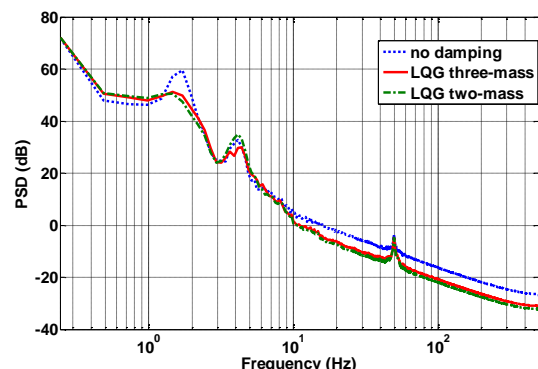


Fig. 10. PSD of LSS torques with/without damping

the three-mass model based damper can mitigate the both torsional vibrations, while the two-mass model based damper can only suppress the vibration with the low frequency and intensifies the other one.

The price for the improved system dynamics is the slightly increased load at very low frequency area, because the LQG is trying to force all system states tend to zero. Fig. 11 shows the torque of the generator. Due to the additional damping torque the generator is a little bit overloaded, which forces the power electronics devices to be overloaded. Usually the 10% is under the tolerance range of the electric devices. Therefore, it will not bring extra hardware cost for the implementation.

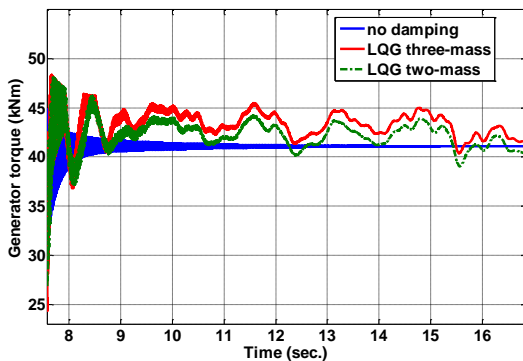


Fig. 11. Generator torques with/without damping (zoomed)

5. Conclusion

This paper proposed a model-based damper of the torsional vibrations of the drive train. The modelling of the drive train takes the symmetrical mode of the blades into account and a three-mass model is applied. The unknown parameters can be derived by the frequency analysis of the load in the drive train. The LQG algorithm is employed to calculate the damping torque. For the active damping only needed measurement of the drive train system is the generator speed. The active damper is tested with a sophisticated wind turbine model realized by different software, in which most important dynamics in mechanical parts and electrical parts are modelled. The results show that the torsional vibrations of the drive train have two dominant frequencies vibrations. The three-mass model based LQG damper can suppress the both effectively. If the standard two-mass model is applied, there is the risk that the torsion oscillation with another frequency can be increased. The proposed damping method does not add any additional hardware to the system and need less online computation. Thus, it can be easily implemented in practice.

References

[1] P. Asmus and M. Seitzler, "The wind energy operation & maintenance report," Nat. Wind Watch, Rowe, MA, Feb. 2010.
 [2] E. Bossanyi, "Wind turbine control for load reduction, Wind Energy, vol. 6, no. 3, pp. 229-244, 2003.
 [3] A. Nasiri, E. Muljadi, G. Mandic, and F. Oyague, "Active Torque Control for Gearbox Load Reduction in a Variable Speed Wind Turbine," IEEE Transactions on Industry Applications, vol. 48, no. 6, pp. 2424-2432, 2012.

[4] F. Zhang, W. Leithead, and O. Anaya-Lara, "Wind turbine control design to enhance the fault ride-through capability," in Renewable Power Generation (RPG 2011), IET Conference on, 2011, pp. 1-6.
 [5] J. M. Jonkman and M. L. Buhl Jr, "FAST user's guide," Golden, CO: National Renewable Energy Laboratory, 2005.
 [6] R. Fadaeinedjad, M. Moallem, and G. Moschopoulos, "Simulation of a wind turbine with doubly fed induction generator by FAST and Simulink," Energy Conversion, IEEE Transactions on, vol. 23, pp. 690-700, 2008.
 [7] J. M. Jonkman, S. Butterfield, W. Musial, and G. Scott, Definition of a 5-MW reference wind turbine for offshore system development: National Renewable Energy Laboratory Colorado, 2009.
 [8] B. Wu, Y. Lang, N. Zargari, and S. Kouro, Power conversion and control of wind energy systems: Wiley-IIEEE Press, 2011.
 [9] F. Iov, A. D. Hansen, P. Sørensen and F. Blaabjerg, "Wind Turbine Blockset in Matlab/Simulink", Report, Aalborg Univeristy, 2004.
 [10] A. Perdana, "Dynamic Models of Wind Turbines", Ph. D thesis, Chalmers University of Technology, 2008.
 [11] R. Lohde, S. Jensen, A. Knop and F. W. Fuchs, "Analysis of three phase grid failure and doubly fed induction generator ride-through using crowbars," in Power Electronics and Applications, 2007 European Conference on, 2007, pp. 1-8.
 [12] L. G. Meegahapola, T. Littler, and D. Flynn, "Decoupled-DFIG fault ride-through strategy for enhanced stability performance during grid faults," Sustainable Energy, IEEE Transactions on, vol. 1, pp. 152-162, 2010.
 [13] A. D. Hansen and G. Michalke, "Fault ride-through capability of DFIG wind turbines," Renewable energy, vol. 32, pp. 1594-1610, 2007.
 [14] G. Ramtharan, N. Jenkins, O. Anaya-Lara and E. Bossanyi, "Influence of rotor structural dynamics representations on the electrical transient performance of FSI and DFIG wind turbines," Wind Energy, vol. 10, pp. 293-301, 2007.
 [15] H. Li and Z. Chen, "Transient stability analysis of wind turbines with induction generators considering blades and shaft flexibility," 33rd Annual Conference of the IEEE in Industrial Electronics Society, 2007, pp. 1604-1609.
 [16] B. J. Jonkman, TurbSim user's guide: Version 1.50: National Renewable Energy Laboratory Colorado, 2009.